Macromolecules

pubs.acs.org/Macromolecules Article

Renewable and Biodegradable Polyurethane Foams with Aliphatic Diisocyanates

Aaron Bruckbauer, Gordon B. Scofield, Marco N. Allemann, Jaysen Reindel, Jiayu Zhao, Ayden N. Howell, Thomas Frisch, Lindsey Johnson, Payton Evans, Robert S. Pomeroy, Ryan Simkovsky, Jinhye Bae, Stephen P. Mayfield, and Michael D. Burkart*

Cite This: *Macromolecules* 2024, 57, 2879–2887 Read Online

ACCESS | Metrics & More | Article Recommendations | Supporting Information

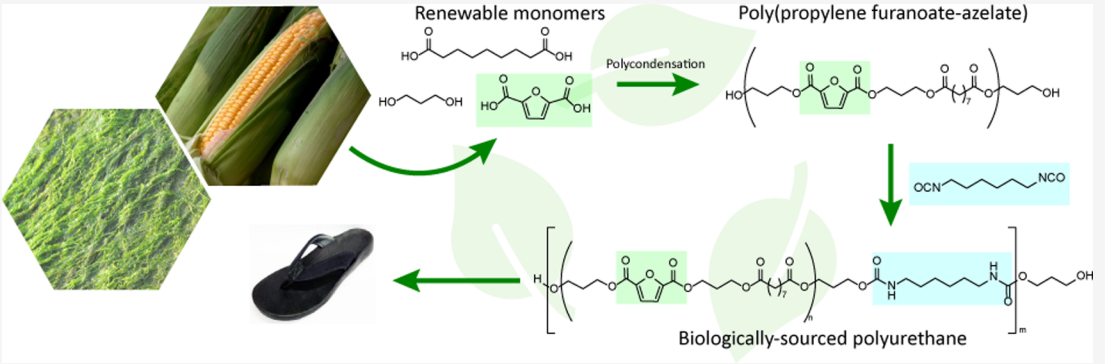

ABSTRACT: The transition to renewable plastics will require the development of substitutes with existing industrial standards and manufacturing processes. Polyurethanes (PU), versatile plastics, are traditionally dominated by aromatic diisocyanates, which are challenging to derive from renewable sources. However, for higher biocontent, it is crucial to utilize aliphatic diisocyanates, which can be sourced from renewable plant or algae waste streams. Historically, PU foams relied on aromatic diisocyanates for essential hard segments, resulting in desired physical properties. Here, we report the generation of high-performance renewable and biodegradable PU foams utilizing aliphatic diisocyanates and aromatic polyols, translating hard segments into the polyester polyol component using biosourced furan dicarboxylic acid (FDCA) monomers. We demonstrate that an FDCA-based PU is suitable for foams with performance characteristics that meet commercial tolerances and can biodegrade under backyard compost conditions. This demonstrates steps toward redesigning traditional petrochemical-based polymers to accommodate new biological monomers.

INTRODUCTION

Today, over half a billion tons of plastics are produced each year from petroleum feedstocks, with <10% recycled globally and <1% considered biodegradable.[1,2] The large majority of plastics are simply discarded, many ending up as environmental contaminates in oceans or incinerated, contributing to greenhouse gas emissions. Polyurethanes (PUs), which account for approximately 10% of global plastic,[3] offer a broad range of material properties, from thermoplastics such as coatings and adhesives to thermosets including construction materials, fashion, and footwear.[4−7] This versatility offers a broad variety of applications that are derived from variation in the two principal components, a polyol and a diisocyanate. Meanwhile, biosourced polyester polyols can be used to replace polyether polyols, offering some renewability benefits. Diisocyanates, the major reactive species, are almost exclusively derived from petroleum today.

With no established renewable replacement, aromatic diisocyanates dominate 90% of PU products,[8,9] and a dogma of PU formulation indicates that aromatic diisocyanates are required for the rigid segments of thermoset foams.[10] Although aliphatic diisocyanates are often used in specialized thermoplastic coatings and adhesives, they have not found broad adoption in commercial PU formulations. We recently reported a scalable route to renewable aliphatic isocyanate, 1,7-heptamethylene diisocyanate (7-HDI), derived from natural lipids and envisioned the potential to prepare fully renewable PU products from aliphatic diisocyanates. Here, we show that aromaticity can be introduced into the polyol side of PU formulations by incorporation of renewable furan dicarboxylic acid (FDCA) in polyol formulations while

Received: November 16, 2023
Revised: February 15, 2024
Accepted: February 27, 2024
Published: March 12, 2024

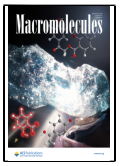

https://doi.org/10.1021/acs.macromol.3c02356
Macromolecules 2024, 57, 2879−2887

utilizing commercially available 1,6-hexamethylene diisocyanate (6-HDI) to demonstrate aliphatic diisocyanates in thermoset polyurethanes for commercial application. The advancement in aliphatic diisocyanate-based polyurethane foams presents an opportunity to develop fully renewable PU foams that are also fully biodegradable.

FDCA is an aromatic monomer sourced from hexose monosaccharides and has been identified as an important renewable building block for future polymer materials.[11] Much of the research on FDCA has focused on poly(ethylene furanoate), an alternative to poly(ethylene terephthalate) (PET) materials, and is currently under commercial development for food and drink packaging. Other research explores copolymerization of FDCA to increase industrial relevance and broaden applications.[12] Recently, the preparation of flame-retardant rigid polyurethane foams using FDCA as an aromatic polyol was reported,[13] but little is known about FDCA's potential in PU foam systems. Here, we utilize FDCA as an aromatic monomer to provide aromatic moieties on the polyol side of PU foam formulations with aliphatic diisocyanates. By moving the aromatic character into the polyol, we produced an aliphatic PU foam that is mechanically robust, thermally stable, and fully biodegradable. This formulation has the potential to be used as a drop-in solution for petroleum-sourced PUs for a variety of commercial products, including footwear applications.

EXPERIMENTAL SECTION

Materials. All of the chemicals received were used without further purification. FDCA (98+%) was supplied from Shandong Ench (Shanghai, China). Azelaic acid (98%) was purchased from Acros Organics (Verona, Veneto), 1,3-propane diol (98%) was purchased from Susterra (Loudon, Tennessee), and dibutyltin dilaurate (DBDTL) catalyst (95%) was purchased from Sigma-Aldrich (St. Louis, Missouri). PU additives (L-1507, Y, DBTDL, and A) were supplied from Momentive (Niskayuna, New York). 1,6-Hexamethylene diisocyanate (98%) was supplied by Alfa Aesar (Haverhill, Massachusetts). The determination of hydroxyl and acid value titrations was performed according to ASTM 1899 and D664, respectively. The reagents used for the titrations were *p*-toluenesulfonyl isocyanate (96%) and 1.0 M tetrabutylammonium hydroxide in methanol, supplied by Sigma-Aldrich (Burlington, Massachusetts). Solvents used for titrations were HPLC grade acetonitrile, toluene, 2-propanol, reagent grade 1-octanol, and potassium hydroxide supplied by Fisher Chemical (Waltham, Massachusetts). Soleic cupsole, here termed cupsole, was supplied by Algenesis Materials (San Diego, California).

General Procedure of Poly(propylene furanoate-azelate) (PPFA). In a typical polycondensation reaction for the FDCA polyol, 2-5-furandicarboxylic acid and 1,3-propane diol were added together in a two-necked round-bottom flask equipped with a magnetic stir bar. A cooled, jacketed reflux condenser was attached to a Dean−Stark apparatus for monitoring of water released from the polymerization reaction under heat, stirring, and a N_2 atmosphere. Once a homogeneous mixture was obtained, azelaic acid was added. Typically, after 8 h, 80% of the expected water byproduct was collected in the Dean−Stark apparatus. Then, catalytic DBTDL was added and polycondensation was continued for typically 48−72 h monitored periodically through acid and hydroxyl number titrations. After the desired acid number was achieved (<1), the polyol was heated in a vacuum oven for 3 days at 90 °C to remove remaining water.

General Preparation for 6-HDI-Based Polyurethane Foam (PPFA-6A). A typical flexible PU foam formulation contained polyol, diisocyanate, a surfactant, and water. Additional additives such as blowing catalyst, gelling catalyst, and dyes can be added to modify the formulation. As a result, there are several variables that play significant roles in product quality. Here, PU foam formulations contained polyol, chain extender, surfactant, water, blowing catalyst, and gelling catalysts that were added to a plastic cup and mixed at 2000 rpm for 1 min in a FlackTek SpeedMixer DAC 600.1 FVZ LR. The mixture was oven-heated to 75 °C and then nucleated with an overhead stirrer equipped with a 3 cm Jiffy Mixer blade. Diisocyanate was added to the polyol mixture, mixed at 2350 rpm for 10 s in the FlackTek SpeedMixer, and then poured into a closed stainless-steel mold heated to 55 °C. Foams were demolded after 24 h and tested for physical and thermal properties after 48 h at room temperature.

Nuclear Magnetic Resonance Spectroscopy (NMR). The ^{1}H and ^{13}C NMR spectra were recorded on a JEOL ECA 400 instrument at ambient temperature. The chemical shifts for the ^{1}H NMR spectra were reported in parts per million relative to the central singlet solvent signal of DMSO at 2.5 ppm. The ^{13}C NMR spectra were reported in ppm relative to the signal of DMSO at 39.5 ppm.

Size Exclusion Chromatography (SEC). Gel permeation chromatography (GPC) was carried out in a Malvern GPC system equipped with Tosoh TSKgel SuperHZM-N and guard columns. The molecular weight and molecular weight distribution of the polymer are relative to a polystyrene standard. THF served as the polymer solvent and eluent with a flow rate of 0.35 mL/min.

Thermal Conductivity Measurements. Dynamic mechanical analyzer (DMA) measurement for TPUs was performed on a TA Instruments DMA 850 with a DMA oscillatory temperature ramp using a 3-point bending clamp in the temperature range of −120 to 120 °C under a nitrogen atmosphere. Differential scanning calorimetry (DSC) analysis was performed on a TA Instruments DSC 2500 from −120 to 220 °C at the rate of 10 °C/min under a nitrogen atmosphere. Thermal gravimetric analysis (TGA) was carried out on TA Instruments Discovery TGA from 50 to 900 °C using a temperature ramp of 10 °C/min under a nitrogen atmosphere.

Mechanical Tests. Viscosity was measured using a Digital Rotary Viscometer at 55 °C with 3 spindles and 30 rpm. Hardness was measured using a Hoto Instruments Asker C Durometer Model E2-C according to ASTM D2240. Tensile strength and elongation at break were measured using a Shimadzu 10 kN Universal Testing Machine (UTM) Model AGS-X with standard flat pneumatic grips Model PFG-10kNA and a California Air Tools Ultra Quiet Air Compressor according to ASTM D3574-17 method E. The strain rate used was 500 mm/min. Tear strength type C was measured using a Shimadzu 10 kN Universal Testing Machine (UTM) Model AGS-X with standard flat pneumatic grips Model PFG-10kNA and a California Air Tools Ultra Quiet Air Compressor according to ASTM D624-00. The strain rate was 500 mm/min. Tear strength type C was measured using a Shimadzu 10 kN Universal Testing Machine (UTM) Model AGS-X with standard flat pneumatic grips Model PFG-10kNA and a California Air Tools Ultra Quiet Air Compressor according to ASTM D624-00. The strain rate was 500 mm/min. The compression set was measured using a Universal Grip Co. compression set test fixture according to ASTM D395 method B. Ten millimeter-thick disks were compressed to 7.50 or 8.20 mm thickness for 6 h at 45 °C and then were allowed to cool to room temperature for 30 min before measurements were taken. DIN abrasion resistance was measured using NextGen DIN Abrasion Tester Model NG-DIN according to ASTM D5963-22. The DIN abrasion tester was set to 84 revolutions. Resilience was measured using a Bareiss GmbH Rebound Elasticity Tester according to ASTM D7121-05. Tensile strength, elongation, tear C strength, compression set, DIN abrasion, and resilience test specimens were all prepared by die-cutting standard testing shapes out of molded 20 × 20 × 1 cm slabs of foam. Die-cutting was performed using a Tippman 15 Ton Clicker 1500 with an air accumulator and a California Air Tools Ultra Quiet Air Compressor. All testing shapes were chosen according to each test's respective ASTM standard. Hysteresis loss and maximum force were measured using a MecMesin MultiTest dV and a 2500 N advanced force gauge (AFG) according to ASTM D3574 method X6. This was performed on 1 in. × 1 in. × 1 in. cubes, which were then compressed to 1/2 of their original height (0.5 in.) using 10 cycles. The first 9 cycles were considered as conditioning, and the data presented were from the 10th cycle.

https://doi.org/10.1021/acs.macromol.3c02356
Macromolecules 2024, 57, 2879−2887

Scheme 1. Synthesis of Polyester Polyol and Polyurethane Foam

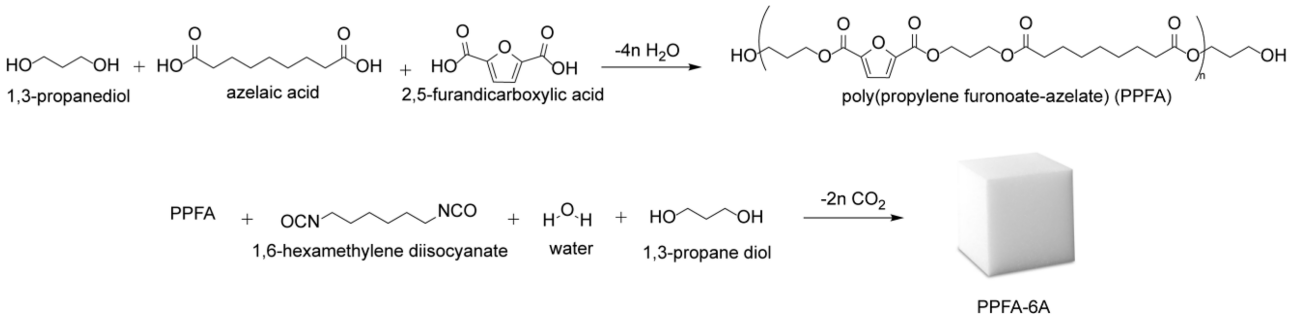

Structural Analysis. FTIR analysis was performed on a PerkinElmer Spectrum X fitted with a ZnSe 1 mm ATR cell; 16 scans were taken at a 1.0 cm^{-1} resolution. The surface topologies of PU foams were characterized by atomic force microscopy (AFM) (Veeco Scanning Probe Microscope) in ambient conditions using tapping mode. Silicon cantilevers and tips (Oxford Instruments) have the force constant of 8.4−57 N/m and the resonance frequency of 200−400 kHz, which were used at a driving frequency of 274 kHz. The foam samples were cut to 10 mm × 10 mm × 2 mm for the imaging. The scanning size was set to 25 × 25 μm^2, and the scanning rate was set to 0.5 Hz. Various foam samples were attached to a 32 mm aluminum SEM sample stub by using carbon tape as the adherent. A Denton Vacuum DESK IV Sputter Coater was used to deposit a thin layer of iridium on the samples. The sputter coater was set to a sputter set point of 95% with a rotation set point of 100% and a 90 s sputter time. All samples were imaged under high vacuum using an FEI Quanta FEG 250 scanning electron microscope at a specified voltage of 5 kV. Images were obtained at magnifications ranging from 100× to 2000× of both the foams' surface and open cell structure. Each sample was visually analyzed for a comparison of structural details. X-ray diffraction (XRD) measurements were carried out to investigate the microstructure difference between PPFA-6A and commercial samples (midsole and insole). XRD profiles of film samples (10 mm × 5 mm × 1 mm) were measured by using an X-ray diffractometer (Anton Paar XRDynamic 500) with Cu Kα radiation (λ = 0.154 nm) running at 40 kV and 49 mA.

Biodegradation Analysis. Biodegradation of PU foams was performed under controlled composting conditions according to the ASTM D5338-15 standard, monitoring CO_2 evolution.[14] Cellulose served as the positive control; ethylene-vinyl acetate (EVA) and compost-only samples served as negative and blank controls, respectively. The experiment was stopped after 200 days of incubation once the mineralization plateau was reached for most materials. For sample preparation, substrates were pelletized into ∼5 mm pieces using an industrial pelletizer. Fresh compost was collected from Roger's Community Garden composting site at UCSD (32.97° N, 117.24° W). Twenty grams of sample material(s) and 240 g of fresh compost were thoroughly mixed, and samples were incubated in a respirometer (Echo Instruments). Sample chambers were maintained at 45 °C and ∼58% relative humidity for the duration of the experiment. Sample chambers were opened biweekly to mix compost and water as needed. The compost experiments were carried out on borosilicate glass dishes packed with composted materials collected and sieved from Rogers Garden at the University of California, San Diego. Samples are added to the soil and maintained for the duration of their digestion at 45 °C at high ∼58% humidity and scheduled for specific time points for postdegradation analysis. Samples were analyzed prior to compost degradation to determine the initial masses and FTIR spectra. Masses were taken via the Mettler Toledo AG204 Analytical Balance, FTIR data were taken via the Nicolet i520 FTIR spectrometer, compression values were obtained via the Mecmesin MultiTest-dV Motorized Force Tester. Fenton's reagent was created by mixing an equivolume (30 mL each) of 30% hydrogen peroxide and an iron sulfate complex. The iron sulfate complex was created by dissolving 7.5 g of iron sulfate heptahydrate in 500 mL of DI water, and then once dissolved, 3 mL of concentrated sulfuric acid was added. The samples were then submerged in Fenton's solution to ensure contact with all biomaterials. After 30 min, the reagent and sample were heated in a water bath to 55 °C, and the heat was then removed as the exothermic reaction catalyzed itself, reaching upward of 75−80 °C during the peak of the reaction before settling back down at 55 °C. The reaction lasted 5 min before cooling down for another 15 min. The sample was then removed from the solution, rinsed of Fenton's reagent, and left to dry overnight in a vacuum desiccator. FTIR, mass, and compression data were repeated to compare to initial nondegraded standards. The samples were maintained weekly via physical sample transfer into a holding container, while the compost was aerated and watered to initial conditions.

RESULTS AND DISCUSSION

Fabrications of PPFA and PPFA-6A Flexible Foam. To obtain poly(propylene furanoate-azelate) (PPFA), a fully biobased aromatic polyester polyol, 1,3-propane diol (PDO) was polymerized with sugar-derived FDCA, and lipid-derived azelaic acid was catalyzed by dibutyltin dilaurate (DBTDL) (Scheme 1). The resulting aromatic polyester polyol was characterized using nuclear magnetic resonance (NMR) and Fourier-transform infrared spectroscopy (FTIR) to confirm its chemical structure, as well as gel permeation chromatography (GPC) to determine the polyol's polydispersity index (PDI) and molecular weight (MW) (Supporting Information, Figures S1−S5). Formation of an ester bond between FDCA and PDO was confirmed by the presence of an ester-attached methylene group from the PDO backbone with a distinguished ester carbonyl group at δ = 172.58 ppm in the ^{13}C NMR spectra and FTIR peaks at 1730 and 1170 cm^{-1}, indicating the formation of the ester carbonyl group. GPC analysis demonstrated that the polyol has a PDI of 1.75 and an M_n of 3467 g/mol. Hydroxyl titration resulted in a value of 65 mg KOH/g, from which a molecular weight of 1680 g/mol was calculated (Supporting Information, eq 1).

The use of multiple diacids in the polyol formulation has been shown to reduce viscosities of polyester polyols, an industrially relevant challenge to ensure that polyester polyols can function in manufacturing equipment typically designed for lower viscosity polyether polyols. Rajput et al. utilized combinations of azelaic acid, sebacic acid, and succinic acid with 1,3-propane diol (PDO) and measured their viscosity and physical state at room temperature. They observed that ratios of alternating chain length of diacids resulted in the greatest viscosity decrease in polyester polyols.[15] Another study by Rhein et al. utilized polyethylene glycol at various equivalences to obtain processable high molecular weight FDCA-based polyols. To lower viscosities even further, they added 10−20 mol % succinic acid or adipic acid to maintain the fully

https://doi.org/10.1021/acs.macromol.3c02356
Macromolecules 2024, 57, 2879−2887

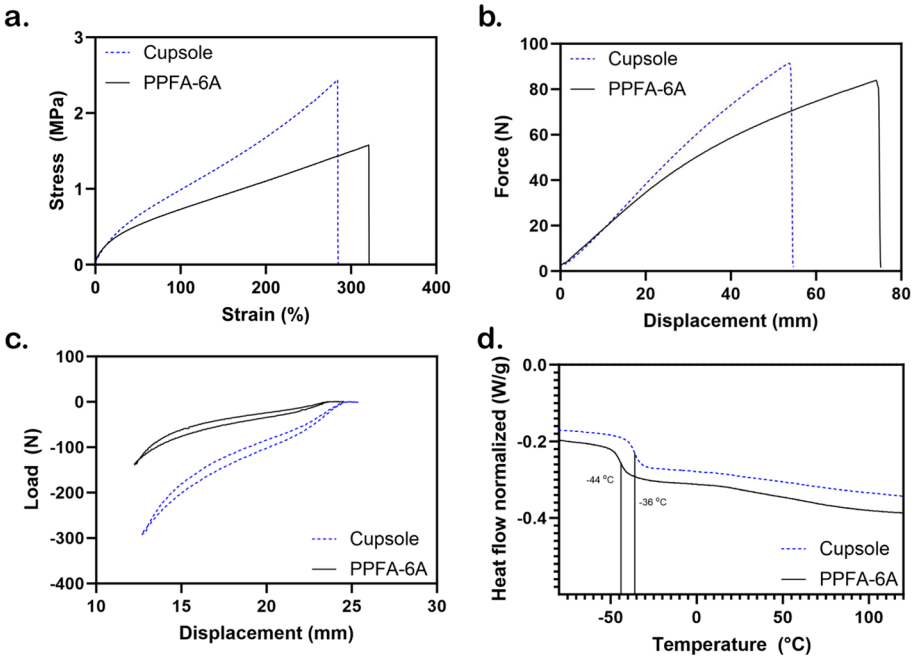

Figure 1. Representative physical property measurements of generated foams. (a) Stress−strain curves measuring material tensile strength and elongation (n = 3, one test shown for simplicity). (b) Force−displacement curve measuring tear c strength (n = 3, one test shown for simplicity). (c) Cyclic force loading demonstrating energy dissipation (n = 10, 10th cycle shown for simplicity). (d) Thermal profile by a differential scanning curve (DSC) (n = 3, one test shown for simplicity).

biobased character of the polyol, which further increased the processability of the FDCA-based polyol.[13] PPFA was subjected to viscosity analysis carried out at 65 °C, resulting in a viscosity of 2380 cP compared to that of the commercial polyol having a viscosity of 2500−2900 cP at 50 °C. While the cP is lower for PPFA at a higher temperature compared to that of the cupsole polyol, PU foam manufacturing can utilize temperatures upward of 80 °C during processing, resulting in an industrially relevant polyester polyol. We hypothesize that the slight increase in viscosity is due to the rigidity of the FDCA monomer in the polyol formulation as a result of steric hindrance and an increase in intermolecular forces such as pi−pi interactions of the aromatic groups, resulting in restricted movement between polymer chains.

The characterized PPFA polyester polyol then underwent subsequent PU synthesis with hexamethylene diisocyanate (6-HDI) and PDO as a chain extender to obtain a PU foam, called here PPFA-6A. Formulation equivalences are described in Supporting Information, Table S1. PPFA showed suitable reactivity compared to that of the commercial flexible foam formulation supplied by Algenesis Materials, which is used exclusively for the footwear industry (Supporting Information, Table S2).

Properties of PPFA-6A Flexible Foam. The mechanical and thermal properties of the flexible PU foam, PPFA-6A, were measured by a variety of instruments and compared against a commercial cupsole foam, which is a flexible PU foam used in the footwear industry, to determine its suitability for a similar commercial application. Our preference for the footwear industry was rationalized by its representation of mechanically demanding material while having a limited product lifetime with many footwear product waste ending up in landfills or oceans or being incinerated.[16] We defined comparable properties to be determined by a range of physical metrics commonly requested by companies in the footwear industry. A universal testing machine was used to investigate tensile tests such as tensile strength, elongation, and tear c, as shown in Figure 1a,b. Energy dissipation of the foam was determined by hysteresis where a 1 in. foam cube was subjected to cyclic compression shown in Figure 1c and Table 1 (Supporting Information, eqs 3 and 4).

Table 1. Stress−Strain-Based Properties of Aliphatic-Based Foam Compared to Commercial Shoe Cupsole

sample name	tensile strength (kg/cm^2)	elongation (%)	tear c strength (kg/cm)	hysteresis (%)
PPFA-6A	15.11 ± 1	299 ± 20	8.64 ± 0.29	81.1
cupsole	24.69 ± 5.29	278 ± 46	9.81 ± 0.81	88.5

Other important mechanical properties, hardness, abrasion resistance, density, compression, and rebound, were determined as shown in Table 2. Glass transition temperature (T_g) was investigated by differential scanning calorimetry (DSC) and determined to be −44 °C shown in Figure 1d with a decomposition temperature (T_d) at 301 °C determined by thermogravimetric analysis (TGA) (Table 2).

All mechanical and thermal characteristics align closely with the established range of metrics employed by the footwear industry, an example being the commercial cupsole presented here. Notably, the PPFA-6A foam has a 3-fold increase in abrasion resistance and a one-third decrease in density relative to the cupsole foam, resulting in less PPFA-6A foam material required to generate the same volume of high-quality polyurethane foam compared to commercially relevant metric standards (Supporting Information, Table S3). Due to a vast range of formulations that can be generated using these same raw ingredients at alternative ratios, resulting in greatly varied foam properties, the potential commercial applications for this foam are diverse.

https://doi.org/10.1021/acs.macromol.3c02356
Macromolecules 2024, 57, 2879−2887

Table 2. Mechanical and Thermal Properties of Aliphatic-Based Foam Compared to Commercial Shoe Cupsole

sample name	DIN abrasion (mm^3)	compression (%)	hardness (Asker C)	rebound (%)	density (kg/cm^3)	T_g (°C)	T_d (°C)
PPFA-6A	32 ± 23	20 ± 2.4	50 ± 3.0	42 ± 2.0	234	−44	301
cupsole	130 ± 70	15.3 ± 0.6	55 ± 3.0	43 ± 0.1	398	−36	309

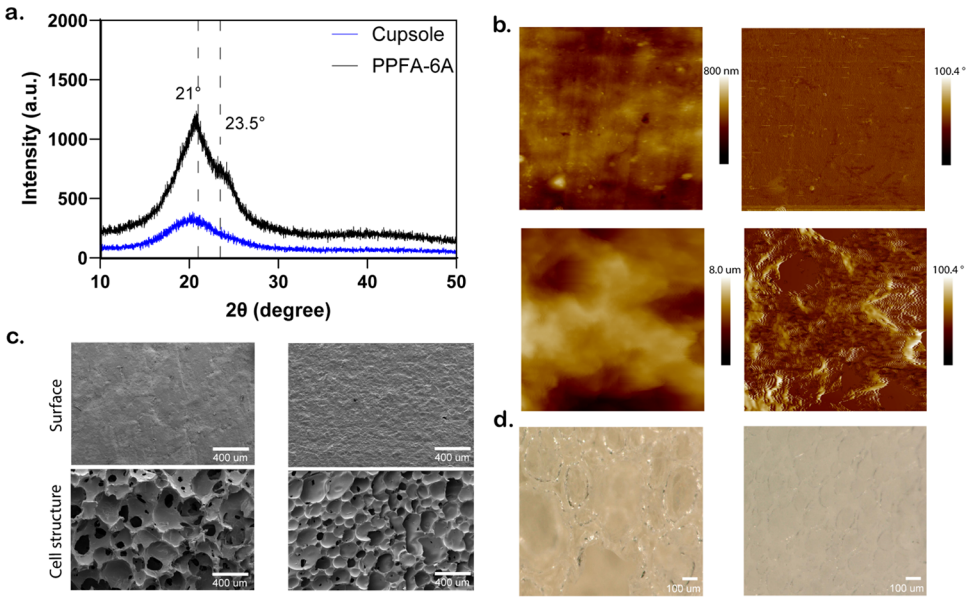

Figure 2. Structural and morphology characteristics of PPFA-6A flexible foam compared with commercial cupsole. (a) Powder X-ray diffraction (XRD) patterns of PPFA-6A and commercial cupsole. (b) Atomic force microscopy (AFM) of the PPFA-6A phase profile (top left) and topography (top right) and cupsole phase profile (bottom left) and topography (bottom right). (c) Scanning electron microscopy (SEM) images of PPFA-6A (top left, bottom left) and cupsole (top right, bottom right) and (d) optical microscopy images of PPFA-6A (left) and cupsole (right).

Structure of PPFA-6A Flexible Foam. PPFA-6A is composed of an aliphatic diisocyanate and has aromatics in the polyol component; instead of the traditional location of aromatics in the isocyanate component, it was unclear how the hard segments would form relative to the historically used aromatic diisocyanate-derived foams. X-ray diffraction (XRD) measurements were carried out to investigate the microstructure of PPFA-6A relative to that of the commercial cupsole. XRD of foam samples was measured, and all samples exhibited a distinct broad diffraction peak at a 2θ angle of 21° (Figure 2a). The interchain spacing "d" can thus be calculated as 4.23 Å using Bragg's law (Supporting Information, eq 5). This peak indicates the presence of a short-range, regularly ordered structure comprised of both hard and soft domains, as well as a disordered structure of the amorphous phase of the PU matrix.[17] In comparison, the PPFA-6A peak is significantly sharpened, suggesting the presence of a well-defined short-range microstructural pattern compared with that of the commercial cupsole.

Surface topologies of PPFA-6A and cupsole PU foams were characterized by atomic force microscopy (AFM) in ambient conditions using tapping mode, where areas of higher rigidity in the sample lead to lower tip−sample adhesion due to reduced energy during tip−sample interactions as compared to soft regions.[18] Thus, PPFA-6A exhibits smaller domain size with a more homogeneous surface compared to the commercial cupsole shown in Figure 2b. It is hypothesized that this smaller and more homogeneous morphology of PPFA-6A is due to the dispersed rigidity caused by the aromatic moieties in the polyester polyol and the hydrogen bonding of the diisocyanate as a result of the urethane functionality, whereas cupsole formulation utilizes a linear polyol contributing only to the soft segment and diisocyanates to the hard segment as traditionally seen in polyurethane systems, resulting in a heterogeneous phase domain. However, both foam systems show distinct hard and soft regions, an important characteristic for polyurethane foams, which is consistent with the XRD-based interpretation of the microstructure of the foam.

Scanning electron microscopy (SEM) and optical images were used to further investigate the morphology and cell structure. PPFA-6A and commercial cupsole are similar in structure; the skin of the foam appears rough with no openings or holes, while the commercial cupsole shows a more heterogeneous topography as shown in AFM (Figure 2c). Both PPFA-6A and cupsole show non-uniform craters and holes throughout the structure of the foam with verification of the open cell structure in both samples. Both PPFA-6A and cupsole formulations have a smooth cell structure with uneven depressions. The commercial cupsole foam has smaller depressions, which is also indicated by the smaller cell size as shown by the optical images in Figure 2d.

Biodegradation of PPFA-6A Flexible Foam. Many studies have demonstrated that a variety of copolyesters, utilizing FDCA at various mol percentages, are biodegradable under composting conditions and even achieved degradation greater than 90%.[19,20] However, the overall biodegradation of FDCA polyesters in thermoset polyurethanes has yet to be explored. We determined that the aliphatic diisocyanate-based polyurethane foams were susceptible to biodegradation under home composting conditions,[21] as confirmed through qualitative and quantitative methods (Figure 3). Foam cubes

https://doi.org/10.1021/acs.macromol.3c02356
Macromolecules 2024, 57, 2879−2887

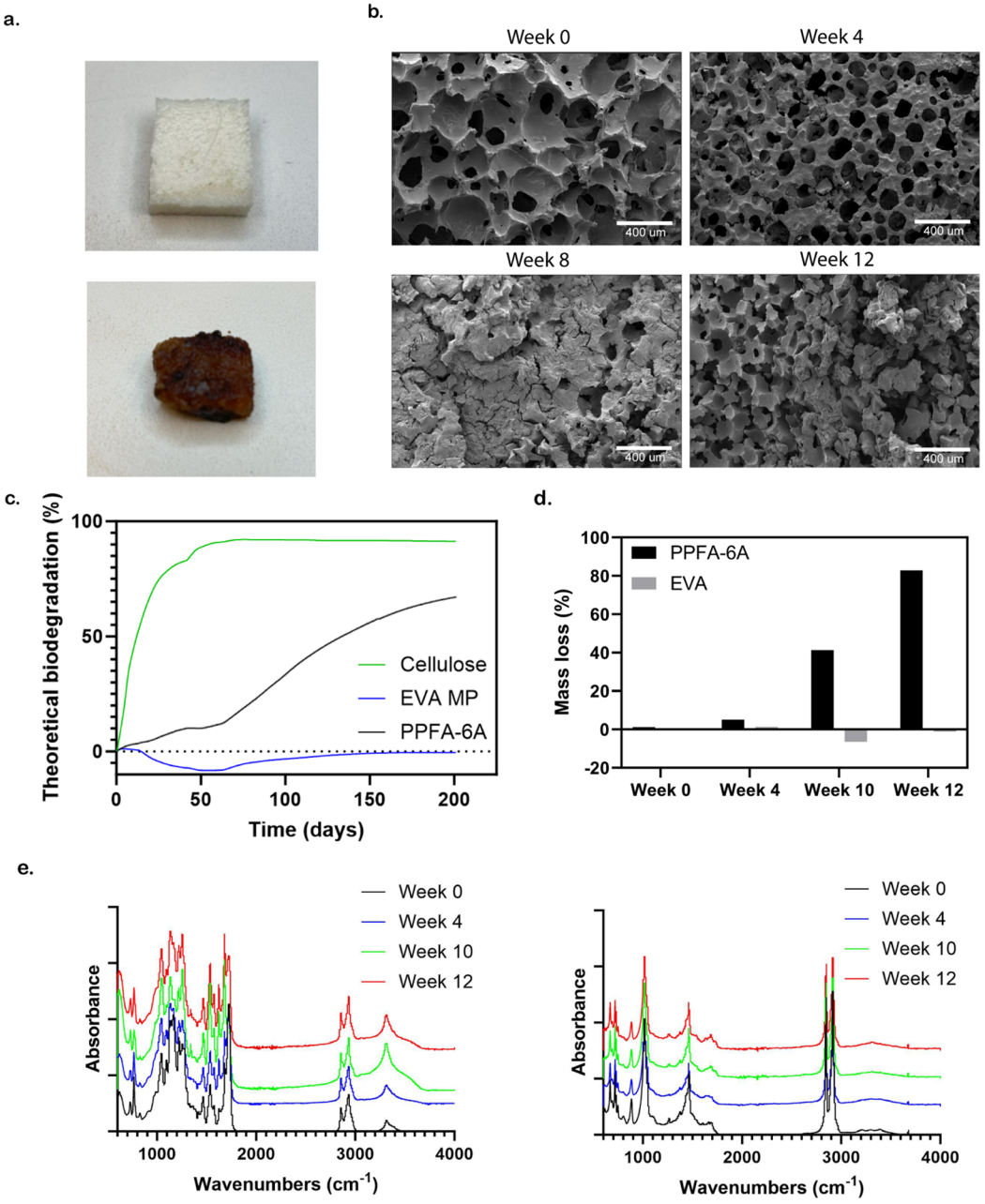

Figure 3. Biodegradation analysis of PPFA-6A. (a) Photographs of PPFA-6A at week 0 (left) and week 12 (right). (b) SEM of PPFA-6A foam samples after 0, 4, 8, or 12 weeks in compost. (c) Respirometry of foam samples over 200 days. (d) Mass loss of PPFA-6A and EVA over 12 weeks in compost. (e) Structural analysis using Fourier transform infrared (FTIR) of PPFA-6A (left) and control ethylene vinyl acetate (EVA) (right) over the course of 12 weeks.

were incubated in compost maintained at 45 °C over the course of 12 weeks. Foam cubes were visually reduced in size and appeared to be discolored over the course of the experiment (Figure 3a). SEM imaging of PPFA-6A at various time points also confirmed structural changes in the foam along with surface-associated microbes compared to the negative control sample of ethyl-vinyl acetate microplastics (EVA MP), a foam known to be nonbiodegradable (Figure 3b).[22,23] Quantitative biodegradation of PPFA-6A was assessed by FTIR, respirometry, and mass loss (Figure 3c–e). The FTIR spectrum of PPFA-6A shows a decrease in signal from week 0 to week 4, and possible structural changes occur at week 10, indicated by a new peak at ~1340 cm^{-1} and an increase in the signal of the hydroxyl and amine stretch at ~3310 cm^{-1}. It is hypothesized that the increase in hydroxyl and amine stretch is due to microorganisms breaking the urethane bond between the carbon–oxygen bond, resulting in an increase in hydroxyl functionality. The control EVA sample indicates no discernible changes over the 12 week biodegradation time period. During the course of 12 weeks, we observed a progressive decline in PPFA-6A mass loss as it underwent degradation, culminating in an 83% total mass reduction by week 12. In contrast, the control sample, EVA, showed no discernible alternations. In a separate experiment, respirometry analysis measuring CO_2 released by the sample is shown in Figure 3d, where PPFA-6A reached 65% biodegradation within 190 days in compost with expected degradation to reach 90% within 250 days based on the linear

https://doi.org/10.1021/acs.macromol.3c02356
Macromolecules 2024, 57, 2879–2887

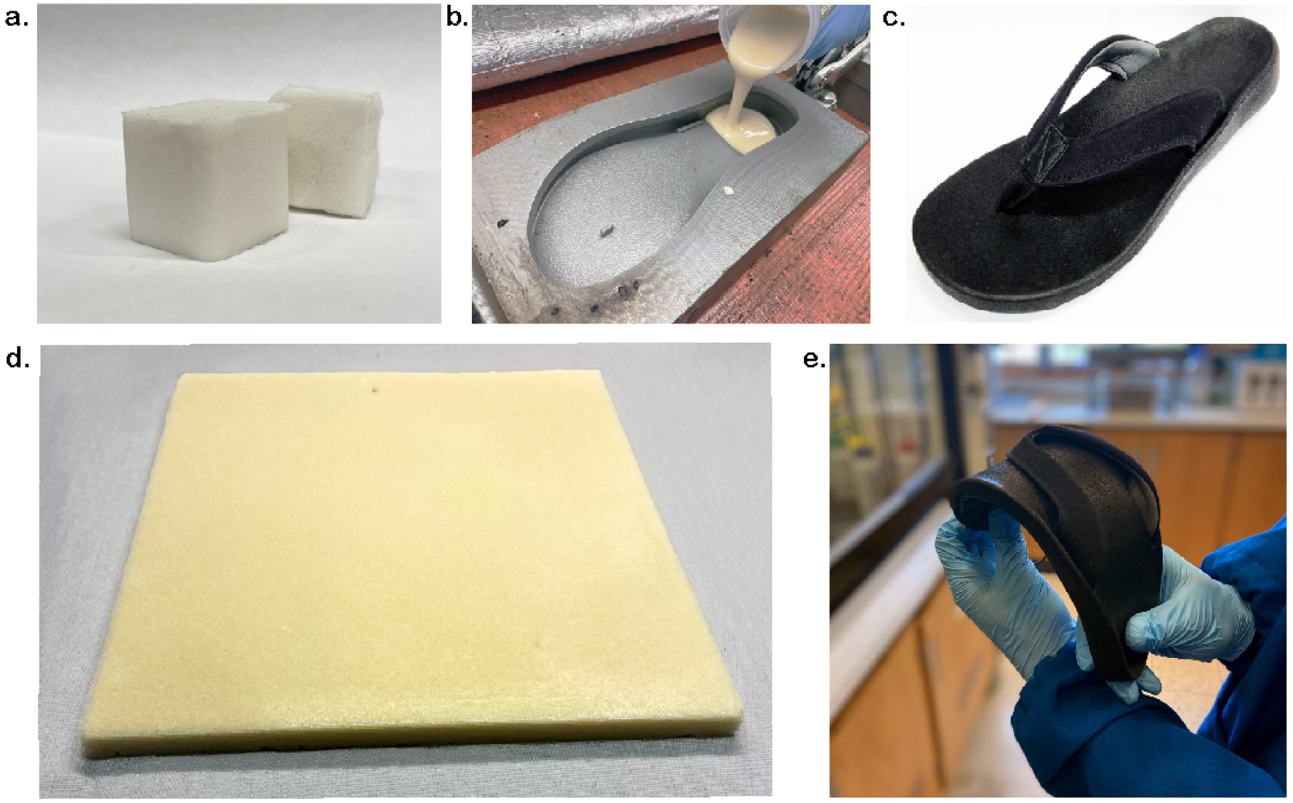

Figure 4. Molded foams of PPFA-6A. (a) Foam after casting into a 1 in. cube mold at 55 °C. (b) The foam was poured into a heated footbed mold at 55 °C. (c) Finalized product using PPFA-6A foam in a footwear application. (d) Foam after casting into a 10 mm slab mold at 55 °C. (e) Demonstration of the flexibility of the finished prototype flip flop product.

trendline (Supporting Information, eq 6). Although this extrapolation is a reasonable estimation of total time for biodegradation for noncomposite-based PU foam systems, it is not a report of a true time frame value. Under identical conditions, the cellulose control sample reached 75% biodegradation within 45 days, consistent with the specifications of ASTM D5338. Respirometry confirms the biodegradation of PPFA-6A by microorganisms to carbon dioxide instead of microplastics while further being supported by the observable change in mass loss, intensity changes of important functional groups, and physical degradation of the material. While the exact degradation mechanism for polyester polyurethane materials has not been elucidated, it is hypothesized that fungi and bacteria release esterase, urease, and urethanase to break down polyester polyurethanes into small molecules. These small molecules, the monomers used in formulation, are then catabolized and taken up by the cell as a carbon source for growth and released in the form of CO_2 when the organism decomposes.[24−26]

Application of PPFA-6A Flexible Foam. With the aforementioned methodology described above for comparative analysis between the novel aliphatic diisocyanate-based foam and the conventional PU foam prevalent in commercial footwear, we successfully executed and demonstrated a potential drop-in solution to achieve 100% biologically sourced PU products with this molecular design. The synthesized aliphatic diisocyanate-based foam, PPFA-6A, was poured into various molds including small cubes, a flip-flop footbed, and thin slabs to demonstrate the versatility of the material (Figure 4a,b,d). The resulting foam from the flip flop mold underwent downstream processing into creating a commercially relevant flip flop. A demonstration of its flexibility is shown in Figure 4c,e.

CONCLUSIONS

Here, we report a novel aliphatic diisocyanate-based polyurethane foam utilizing 100%-biobased polyester polyurethanes incorporating sugar-derived 2,5-furandicarboxylic acid. The synthesized polyol was characterized using proton and carbon NMR spectroscopy, GPC, and FTIR. The prepared polyester polyol showed low viscosity behavior at 65 °C, making it suitable for industrial manufacturing, which allowed testing of aliphatic diisocyanate-based polyurethane foams. These foams were characterized using a variety of structural, thermal, and mechanical techniques, including AFM, DSC, and cyclic loading tests. The novel polyurethane foam displayed excellent thermal and mechanical properties, showing comparable properties to commercial polyurethane foams used in the footwear industry. Detailed structural and morphology investigations show morphologies and structural characteristics similar to those of a commercial PU foam. In addition, the novel foam biodegrades under home composting conditions with the generation of CO_2 as the breakdown product. Further, we also demonstrated proof of application that these PUs could be rapidly implemented into product manufacturing as a drop-in replacement for existing petroleum-based PU foams. This milestone achievement in PU chemistry and formulation calls into question the central dogma of commercial PUs and signifies a progressive move toward renewable products in PU, paving the way for fully sustainable PU materials.

https://doi.org/10.1021/acs.macromol.3c02356
Macromolecules 2024, 57, 2879−2887

■ ASSOCIATED CONTENT

Supporting Information

The Supporting Information is available free of charge at https://pubs.acs.org/doi/10.1021/acs.macromol.3c02356.

Additional materials, methods, equations, and experimental results including ^{1}H, ^{13}C, FTIR, and GPC data for PPFA and raw mechanical and thermal characterization of materials (PDF)

■ AUTHOR INFORMATION

Corresponding Author

Michael D. Burkart − *Department of Chemistry and Biochemistry, University of California San Diego, La Jolla, California 92093, United States;* orcid.org/0000-0002-4472-2254; Phone: 858-534-5673; Email: mburkart@ucsd.edu

Authors

Aaron Bruckbauer − *Department of Chemistry and Biochemistry, University of California San Diego, La Jolla, California 92093, United States*

Gordon B. Scofield − *Algenesis Corporation, San Diego, California 92121, United States*

Marco N. Allemann − *Algenesis Corporation, San Diego, California 92121, United States*

Jaysen Reindel − *Algenesis Corporation, San Diego, California 92121, United States*

Jiayu Zhao − *Jacobs School of Engineering, University of California San Diego, La Jolla, California 92093, United States*

Ayden N. Howell − *Department of Chemistry and Biochemistry, University of California San Diego, La Jolla, California 92093, United States*

Thomas Frisch − *Department of Chemistry and Biochemistry, University of California San Diego, La Jolla, California 92093, United States*

Lindsey Johnson − *Algenesis Corporation, San Diego, California 92121, United States*

Payton Evans − *Department of Chemistry and Biochemistry, University of California San Diego, La Jolla, California 92093, United States*

Robert S. Pomeroy − *Department of Chemistry and Biochemistry, University of California San Diego, La Jolla, California 92093, United States;* orcid.org/0000-0002-9787-1050

Ryan Simkovsky − *Algenesis Corporation, San Diego, California 92121, United States*

Jinhye Bae − *Jacobs School of Engineering, University of California San Diego, La Jolla, California 92093, United States;* orcid.org/0000-0002-2536-069X

Stephen P. Mayfield − *Department of Biology, University of California San Diego, La Jolla, California 92093, United States*

Complete contact information is available at: https://pubs.acs.org/10.1021/acs.macromol.3c02356

Author Contributions

The manuscript was written through contributions of all authors. All authors have been given approval to the final version of the manuscript.

Notes

The authors declare the following competing financial interest(s): M.D.B., R.S.P., and S.P.M. are co-founders and advisors and hold equity in Algenesis materials, a biotechnology company developing commercial products from renewable sources.

■ ACKNOWLEDGMENTS

We are grateful to the University of California, San Diego, Materials Research Science and Engineering Center (UCSD MRSEC), supported by the National Science Foundation under award no. DMR 2011924. The use of facilities and instrumentation supported by the National Science Foundation through the UCSD MRSEC is also gratefully acknowledged. The authors also thank Dr. Rachel Behrens, Dr. Amanda Strom, and Dr. Cesar Rodriguez from Material Research Laboratory (MRL), University of California Santa Barbara (UCSB) for assistance with the analysis of GPC, DSC, DMA, and TGA. The MRL shared experimental facilities supported by the MRSEC program of the NSF under award no. DMR 2308708 as a member of the NSF-funded materials research facilities network (www.mrfn.org).

■ REFERENCES

(1) Agrawala, S.; Mont, N. *In Global Outlook: Economic Drivers*, OCED Publishing, Environmental Impacts and Policy Options, 2022; pp 16−30.

(2) Rosenboom, J.-G.; Langer, R.; Traverso, G. Bioplastics for a Circular Economy. *Nature Reviews Materials* **2022**, *7* (2), 117−137.

(3) Liang, C.; Gracida-Alvarez, U. R.; Gallant, E. T.; Gillis, P. A.; Marques, Y. A.; Abramo, G. P.; Hawkins, T. R.; Dunn, J. B. Material Flows of Polyurethane in the United States. *Environmental Science & Technology* **2021**, *55* (20), 14215−14224.

(4) Ionescu, M. Polyester Polyols for Elastic Polyurethanes. *Chem. Technology Polyols polyurethanes* **2005**, 263−294.

(5) Pourahmady, N. Coatings, Adhesives, and Sealants from Polyester Polyurethanes. *Rethinking Polyester Polyurethanes* **2023**, 195−213.

(6) Neelakantan, N. Polyurethanes: Foams and Thermoplastics. *Rethinking Polyester Polyurethanes* **2023**, 179−194.

(7) Das, A.; Mahanwar, P. A Brief Discussion on Advances in Polyurethane Applications. *Advanced Industrial and Engineering Polymer Research* **2020**, *3* (3), 93−101.

(8) Allport, D. C.; Gilbert, D. S.; Outterside, S. M. *In MDI and TDI: Safety, Health and the environment: A source book and practical guide*; Wiley, 2003; pp 11−23.

(9) Williams, M.; Todd, D.; Pohl, H.; Taylor, J.; Ingerman, L.; Carlson-Lynch, H.; Hard, C.; Citra, M. Toxicological Profile for Toluene Diisocyanate and Methylenediphenyl Diisocyanate. *Cent. Dis. Control Prev.* **2015**, 131−139.

(10) Corcuera, Ma. A.; Rueda, L.; Saralegui, A.; Martín, Ma. D.; Fernández-d'Arlas, B.; Mondragon, I.; Eceiza, A. Effect of Diisocyanate Structure on the Properties and Microstructure of Polyurethanes Based on Polyols Derived from Renewable Resources. *J. Appl. Polym. Sci.* **2011**, *122* (6), 3677−3685.

(11) de Jong, E.; Visser, H. R. A.; Dias, A. S.; Harvey, C.; Gruter, G. J. M. The Road to Bring FDCA and PEF to the Market. *Polymers* **2022**, *14* (5), 943.

(12) Terzopoulou, Z.; Papadopoulos, L.; Zamboulis, A.; Papageorgiou, D. G.; Papageorgiou, G. Z.; Bikiaris, D. N. Tuning the Properties of Furandicarboxylic Acid-Based Polyesters with Copolymerization: A Review. *Polymers* **2020**, *12* (6), 1209.

(13) Rhein, M.; Demharter, A.; Felker, B.; Meier, M. A. A Fully Biobased Aromatic Polyester Polyol for Polyisocyanurate Rigid Foams: Poly(Diethylene Furanoate). *ACS Applied Polymer Materials* **2022**, *4* (9), 6514−6520.

(14) ASTM D5338−15 (2021): Standard Test Method for Determining Aerobic Biodegradation under Controlled Composting Conditions, Incorporating Thermophilic Temperatures. https://www.astm.org/d5338-15r21.html January 20, 2021.
(15) Rajput, B. S.; Hai, T. A.; Gunawan, N. R.; Tessman, M.; Neelakantan, N.; Scofield, G. B.; Brizuela, J.; Samoylov, A. A.; Modi, M.; Shepherd, J.; Patel, A.; Pomeroy, R. S.; Pourahmady, N.; Mayfield, S. P.; Burkart, M. D. Renewable Low Viscosity Polyester-Polyols for Biodegradable Thermoplastic Polyurethanes. *J. Appl. Polym. Sci.* **2022**, *139* (43), No. e53062, DOI: 10.1002/app.53062.
(16) Zhang, Z.; Wei, X.; Wu, H.; Wang, Q.; Zheng, W.; Tang, X. The Present Situation of the Old Shoes Recycling and the Existing Old Shoes Treatment Method. *IOP Conference Series: Materials Science and Engineering* **2018**, *382*, No. 032055.
(17) Barick, A. K.; Tripathy, D. K. Preparation, Characterization and Properties of Acid Functionalized Multi-Walled Carbon Nanotube Reinforced Thermoplastic Polyurethane Nanocomposites. *Mater. Sci. Eng., B* **2011**, *176* (18), 1435−1447.
(18) Lan, Q.; Haugstad, G. Characterization of Polymer Morphology in Polyurethane Foams Using Atomic Force Microscopy. *J. Appl. Polym. Sci.* **2011**, *121* (5), 2644−2651.
(19) Fei, X.; Wang, J.; Zhang, X.; Jia, Z.; Jiang, Y.; Liu, X. Recent Progress on Bio-Based Polyesters Derived from 2,5-Furandicarboxylic Acid (FDCA). *Polymers* **2022**, *14* (3), 625.
(20) Peng, S.; Wu, L.; Li, B.-G.; Dubois, P. Hydrolytic and Compost Degradation of Biobased PBSF and PBAF Copolyesters with 40−60 Mol% BF Unit. *Polym. Degrad. Stab.* **2017**, *146*, 223−228.
(21) Mouhoubi, R.; Lasschuijt, M.; Carrasco, S. R.; Gojzewski, H.; Wurm, F. R. End-of-life biodegradation? how to assess the composting of polyesters in the lab and the field. *Waste Manage.* **2022**, *154*, 36−48, DOI: 10.1016/j.wasman.2022.09.025.
(22) Gunawan, N. R.; Tessman, M.; Zhen, D.; Johnson, L.; Evans, P.; Clements, S. M.; Pomeroy, R. S.; Burkart, M. D.; Simkovsky, R.; Mayfield, S. P. Biodegradation of Renewable Polyurethane Foams in Marine Environments Occurs through Depolymerization by Marine Microorganisms. *Science of The Total Environment* **2022**, *850*, No. 158761.
(23) Sessini, V.; Arrieta, M. P.; Raquez, J.-M.; Dubois, P.; Kenny, J. M.; Peponi, L. Thermal and Composting Degradation of EVA/Thermoplastic Starch Blends and Their Nanocomposites. *Polym. Degrad. Stab.* **2019**, *159*, 184−198.
(24) Gunawan, N. R.; Tessman, M.; Schreiman, A. C.; Simkovsky, R.; Samoylov, A. A.; Neelakantan, N. K.; Bemis, T. A.; Burkart, M. D.; Pomeroy, R. S.; Mayfield, S. P. Rapid Biodegradation of Renewable Polyurethane Foams with Identification of Associated Microorganisms and Decomposition Products. *Bioresource Technology Reports* **2020**, *11*, No. 100513.
(25) Howard, G. T.; Blake, R. C. Growth of Pseudomonas Fluorescens on a Polyester−Polyurethane and the Purification and Characterization of a Polyurethanase−Protease Enzyme. *International Biodeterioration & Biodegradation* **1998**, *42* (4), 213−220.
(26) Gautam, R.; Bassi, A. S.; Yanful, E. K.; Cullen, E. Biodegradation of Automotive Waste Polyester Polyurethane Foam Using Pseudomonas Chlororaphis Atcc55729. *International Biodeterioration & Biodegradation* **2007**, *60* (4), 245−249.

https://doi.org/10.1021/acs.macromol.3c02356
Macromolecules 2024, 57, 2879−2887